arXiv:quant-ph/0608163v2 18 Apr 2007

Transverse Entanglement Migration in Hilbert Space

K.W. Chan,[1] J.P. Torres,[2] and J.H. Eberly[3]

[1]*The Institute of Optics, University of Rochester, Rochester, NY 14627 USA*
[2]*ICFO-Institut de Ciències Fotóniques, and Department of Signal Theory and Communications, Universitat Politècnica de Catalunya, Barcelona, Spain*
[3]*Department of Physics and Astronomy, University of Rochester, Rochester, NY 14627 USA*

We show that, although the amount of mutual entanglement of photons propagating in free space is fixed, the type of correlations between the photons that determine the entanglement can dramatically change during propagation. We show that this amounts to a migration of entanglement in Hilbert space, rather than real space. For the case of spontaneous parametric down conversion, the migration of entanglement in transverse coordinates takes place from modulus to phase of the bi-photon state and back again. We propose an experiment to observe this migration in Hilbert space and to determine the full entanglement.

Entanglement is one of the truly central features of the quantum world, and it forms the core of many applications based on quantum theory. The observation of entanglement is generally achieved through the measurement of correlations between entangled subsystems. Correlation in quantum systems takes many forms and is open to observation in a variety of ways. Therefore, the determination of the amount of entanglement of quantum states depends on the measurement of the correlations where entanglement resides. This is of paramount importance, since in some experimental configurations one registers types of correlation that might not be appropriate to quantify the entangled nature of the quantum state.

In this Communication, we show that the measurement of correlation between paired photons can miss the detection of entanglement entirely. The underlying reason is an interesting migration of entanglement that occurs in Hilbert space, but that depends on coordinate location in real space. This is manifest in photon correlations that show a rich and complex structure that evolves during propagation, although the amount of entanglement is constant. We focus here on entanglement that can become partly or entirely identified with the phase of the state, in which case the measurement of intensity correlations partially or completely misses the existing entanglement. This is an observable manifestation of the "phase entanglement" previously noted [1] for massive particle breakup in an Einstein-Podolsky-Rosen (EPR) scenario.

Entangled photons generated in spontaneous parametric down-conversion (SPDC) are particularly open to the observation of this phenomenon. The generated two-photon states have been shown to exhibit entanglement in transverse momentum [2] and in orbital angular momentum [3, 4]. Moreover, one can enlarge the Hilbert space of the two-photon state by using several degrees of freedom [5]. The spatial transverse degrees of freedom of photon pairs produced in SPDC have attracted great attention because of the vast Hilbert space involved [6, 7], and the availability of techniques to implement the d-dimensional quantum channel [8, 9, 10].

Observations of SPDC entanglement have usually been made either in the near zone or the far zone [11]. Interestingly, in the course of photon propagation from the near field zone to the far field zone, the entanglement embedded in the two-photon positional amplitude migrates out of the positional wave function's modulus into its phase, and then back again.

In the region between near and far zones, the entanglement not obtained through the measurement of intensity correlations can be recovered by measuring the phase information of the joint wave function. Here we propose an experimental setup to accomplish this by exploiting the symmetries of the wave function.

We consider a nonlinear optical crystal of length L, illuminated by a quasi-monochromatic laser pump beam, propagating in the z direction. The signal and idler photons generated propagate from the output face of the nonlinear crystal under the sole effect of diffraction. The quantum state of the two-photon pair generated in SPDC, at a distance z from the output face of the nonlinear crystal ($z = 0$), reads in wave number space as $|\Psi(z)\rangle = \int d\vec{p}\, d\vec{q}\ \ \Phi(\vec{p},\vec{q},z)\ a_s^\dagger(\vec{p}) a_i^\dagger(\vec{q})|0,0\rangle$, where $\vec{p}$ and $\vec{q}$ are the transverse wave numbers of the signal and idler photons, and $a_s^\dagger(\vec{p})$ and $a_i^\dagger(\vec{q})$ are the corresponding creation operators. The signal and idler photons are assumed to be monochromatic. This assumption is justified by the use of narrow band interference filters in front of the detectors.

Under conditions of collinear propagation of the pump, signal and idler photons with no Poynting vector walk-off, which would be the case of a noncritical type-II quasi-phase matched configuration, the mode function $\Phi(\vec{p},\vec{q},z)$ is given by

$$\Phi(\vec{p},\vec{q},z) \ = \ N E_p(\vec{p}+\vec{q})\ \mathrm{sinc}\Big(\frac{\Delta_k L}{2}\Big) \exp\Big(i\frac{s_k L}{2}\Big) \times \exp\{i\,[k_s(\vec{p}) + k_i(\vec{q})]\ z\}, \qquad (1)$$

where N is a normalization factor, $\Delta_k = k_p(\vec{p}+\vec{q}) - k_s(\vec{p}) - k_i(\vec{q})$ and $s_k = k_p(\vec{p}+\vec{q}) + k_s(\vec{p}) + k_i(\vec{q})$, E_p is the transverse profile of the pump at the input face of the nonlinear crystal, and k_j ($j = p, s, i$) are wave number for the pump, signal, and idler waves. We have also made use of the paraxial approximation to describe the propagation of the signal and idler photons in free space.

The sinc function that appears in Eq. (1) can be approximated by a Gaussian exponential function which accurately retains the main features of the entanglement of the wave function [7]. We take $\operatorname{sinc} bx^2 \simeq \exp[-\alpha b x^2]$ with $\alpha = 0.455$, so that both functions coincide at the $1/e^2$ intensity. Here we assume a pump beam with a Gaussian shape. Therefore, the mode function can be written as [12, 13]

$$\Phi(\vec{p},\vec{q},z) = N\exp\left\{-\frac{1}{4}\left[\frac{w_0^2}{1+w_0^4/\sigma_0^2}+i\mu_1(z)\right]|\vec{p}+\vec{q}|^2\right\} \times\exp\left\{-\frac{1}{4}\left[\frac{\alpha L}{k_p^0}+i\mu_2(z)\right]|\vec{p}-\vec{q}|^2\right\}, \qquad (2)$$

where $N = \left\{(w_0^2\alpha L)/[\pi^2(1+w_0^4/\sigma_0^2)k_p^0]\right\}^{1/4}$, $\mu_1(z) = 2(z+L)/k_p^0 - \sigma_0/(1+\sigma_0^2/w_0^4)$ and $\mu_2(z) = (2z+L)/k_p^0$. We denote w_0 as the pump beam width and $\sigma_0 = -2R/k_p^0$, with R being the radius of curvature of the Gaussian beam at the entrance face of the nonlinear crystal and $k_p^0 = \omega_p n_p/c$. ω_p and n_p are the corresponding angular frequency and refractive index, respectively. Notice that we have made use of the approximation $k_p^0 \simeq 2k_s^0 = 2k_i^0$. Moreover, all phase factors independent of the transverse variables have been neglected.

Equation (2) describes the two-photon quantum state in transverse wave number space $(\vec{p},\vec{q})$. We can also describe the two-photon quantum state in coordinate space. In this case, $\Psi(\vec{x}_s,\vec{x}_i,z) = 1/(2\pi)^2\int d\vec{p}\, d\vec{q}\;\; \Phi(\vec{p},\vec{q},z)\exp(i\vec{p}\cdot\vec{x}_s + i\vec{q}\cdot\vec{x}_i)$, and since Eq. (2) can be written as $\Phi(\vec{p},\vec{q},z) = F(\vec{p}+\vec{q},z)G(\vec{p}-\vec{q},z)$, one can easily obtain

$$\Psi(\vec{x}_s,\vec{x}_i,z) = N'\exp\left\{-\frac{1}{4\beta(z)}\left[\frac{\alpha L}{k_p^0}-i\mu_2(z)\right]|\vec{x}_s-\vec{x}_i|^2\right\} \times\exp\left\{-\frac{1}{4\gamma(z)}\left[\frac{w_0^2}{1+w_0^4/\sigma_0^2}-i\mu_1(z)\right]|\vec{x}_s+\vec{x}_i|^2\right\}, \qquad (3)$$

where $N' = N/(\gamma\beta)^{1/4}$, $\beta(z) = (\alpha L/k_p^0)^2 + \mu_2^2(z)$, and $\gamma(z) = w_0^4/(1+w_0^4/\sigma_0^2)^2 + \mu_1^2(z)$. The conditional coincidence rate in coordinate space is given by $\mathcal{R}_x(\vec{x}_s,\vec{x}_i,z) = |\Psi(\vec{x}_s,\vec{x}_i,z)|^2$, while the conditional coincidence rate in momentum space is $\mathcal{R}_p(\vec{p},\vec{q},z) = |\Phi(\vec{p},\vec{q},z)|^2$.

Equation (2) shows that the two-photon state is separable in momentum space, and in coordinate space, if the conditions $w_0^2/(1+w_0^4/\sigma_0^2) = \alpha L/k_p^0$ and $\sigma_0/(1+\sigma_0^2/w_0^4) = L/k_p^0$ are fulfilled, which corresponds to separability in modulus and phase. Notwithstanding, from Eq. (3) we also observe that it is possible that the bi-photon function is separable in modulus at a specific location, although not in phase. Therefore, $|\Psi(\vec{x}_s,\vec{x}_i,z_0)|^2 = |\Psi_s(\vec{x}_s,z_0)|^2|\Psi_i(\vec{x}_i,z)|^2$.

The central point is that, at a certain location z_0 from the output face of the nonlinear crystal, where the z-dependent condition $k_p^0 w_0^2\beta(z_0) = (1+w_0^4/\sigma_0^2)\alpha L\gamma(z_0)$ is fulfilled, one does not observe intensity correlations at all in coordinate space, although the quantum state is not separable in either momentum or coordinate. Since the amount of entanglement is determined by the existing correlations of the bi-photon function in modulus and phase, at z_0 all entanglement lives in the phase of the bi-photon function in coordinate space.

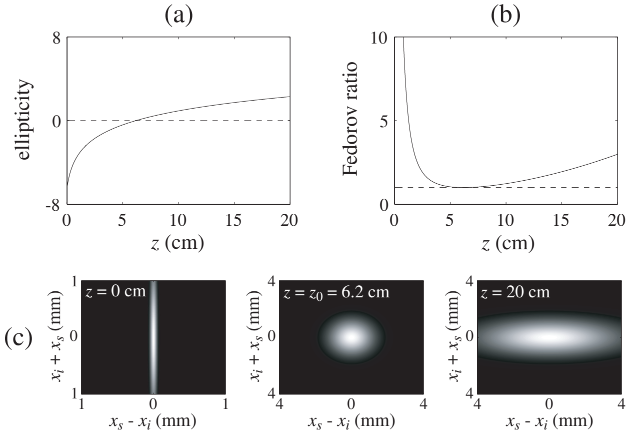

FIG. 1: (a) Ellipticity of the bi-photon function in coordinate space. (b) Fedorov ratio $\mathcal{F}_x$ in coordinate space. The dashed line corresponds to $\mathcal{R}_x = 1$. (c) The spatial conditional coincidence rate $\mathcal{R}_x(\vec{x}_s,\vec{x}_i,z)$ at different locations: $z = 0\,$cm, $z = z_0 = 6.2\,$cm and at $z = 20\,$cm. Parameters: Crystal length $L = 5\,$mm; pump beam width $w_0 = 800\,\mu$m; pump beam wavelength $\lambda_p = 800\,$nm. The ellipticity is plotted in logarithmic scale.

Figure 1(a) shows the evolution of the intensity correlations as a function of the distance z. We plot the ellipticity (e) in the plane $(\vec{x}_s+\vec{x}_i,\, \vec{x}_s-\vec{x}_i)$ of the bi-photon function given by Eq. (3), i.e., $e = k_p^0 w_0^2\beta/[(1+w_0^4/\sigma_0^2)\alpha L\gamma]$. The spatial conditional coincidence rate $\mathcal{R}_x(\vec{x}_s,\vec{x}_i,z)$ for three specific locations z are also shown in the figure. Note that the amount of entanglement does not depend on the location z, while the magnitude of the intensity correlations evolves with z, as shown by the variation of ellipticity in Fig. 1. Therefore, although the amount of entanglement is unchanged with z, the type of correlation that determines the entanglement is different at every location z.

In order to quantify the amount of entanglement of the two-photon state, we perform the Schmidt decomposition [14, 15] of the bi-photon function given by Eq. (2) at the output face of the nonlinear crystal. As shown in Appendix A, the amount of entanglement denoted K (i.e., the Schmidt number for continua [14]) is given by

$$K = \frac{[\Re(A+B)]^2 + [\Im(A-B)]^2}{[\Re(A+B)]^2 - [\Re(A-B)]^2}, \qquad (4)$$

where $A = w_0^2/(1+w_0^4/\sigma_0^2) + i\mu_1$ and $B = \alpha L/k_p^0 + i\mu_2$. Note that K does not depend on z even though μ_1 and μ_2 do so.

For the sake of comparison, let us consider the Fedorov ratio [16], here denoted $\mathcal{F}$, a typical correla-

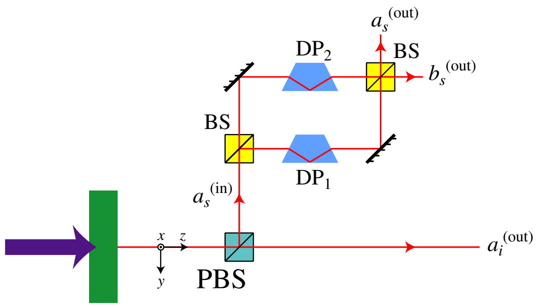

FIG. 2: (Color online) Experimental scheme to detect the total entanglement. The signal photon is directed into a modified Mach-Zehnder interferometer with two Dove prisms DP$_i$ with orientation angles θ_i. PBS is a polarization beam splitter.

tion measurement that could potentially be employed to show the existence of entanglement. For the signal photon in momentum space it takes the form $\mathcal{F}_{s,p} \equiv \langle \Delta^2 \vec{p}_s \rangle / \langle \Delta^2 \vec{p}_s \rangle_i$, and the expression in coordinate space is $\mathcal{F}_{s,x} \equiv \langle \Delta^2 \vec{x}_s \rangle / \langle \Delta^2 \vec{x}_s \rangle_i$. Here the variance averages not containing subscript i are unconditional. The averages with subscript i are conditioned on the idler photon, which is to be constrained by $\vec{p}_i = 0$ and $\vec{x}_i = 0$, in the $\vec{p}_s$ and $\vec{x}_s$ averages respectively.

If the entanglement resides only in the modulus of the bi-photon given by Eq. (2), i.e., $\mu_1 = \mu_2$, $\mathcal{F}_p$ can be shown to be equal to the amount of entanglement given by Eq. (4), while $\mathcal{F}_x$ only gives the correct amount of entanglement in the near and far fields. This is the typical experimental condition if the pump beam shows no curvature at the input face of the nonlinear crystal.

If part or all the entanglement resides in the phase of the bi-photon, even $\mathcal{F}_p$ does not correctly measure the amount of the entanglement of the quantum state, only the part of the entanglement that resides in the modulus of the bi-photon function. Figure 1(b) shows the Fedorov ratio in coordinate space for a typical case. At $z = z_0$, where the bi-photon function shows no ellipticity in the modulus, we have $\mathcal{F}_x = 1$, although the quantum state is entangled.

In Fig. 2 we show an experimental scheme to detect the total entanglement of the bi-photon described by Eqs. (2) or (3). The signal photon is sent to a modified Mach-Zehnder interferometer with two Dove prisms inserted in the interfering arms. The arms are assumed to be balanced so that the relative phase shift between the two arms of the interferometer due to propagation is zero.

We set the orientation angles of the Dove prisms $\theta_1 = \pi/2$ and $\theta_2 = 0$. The conditional coincidence rates of the output ports of the interferometer shown in Fig. 2 take the form (see Appendix B)

$$P_+ = \iint d\vec{x}_s \, d\vec{x}_i \; P_{a_s,a_i}(\vec{x}_s, \vec{x}_i) = \frac{1}{2}\left(1 + \frac{1}{K}\right), \quad \text{(5a)}$$

$$P_- = \iint d\vec{x}_s \, d\vec{x}_i \; P_{b_s,a_i}(\vec{x}_s, \vec{x}_i) = \frac{1}{2}\left(1 - \frac{1}{K}\right), \quad \text{(5b)}$$

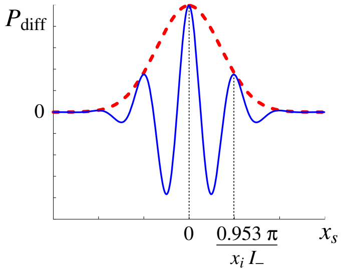

FIG. 3: (Color online) The coincidence interference pattern observed in the setup of Fig. 2. The dotted line shows the situation when phase entanglement is absent.

where

$$P_{a_s,a_i}(\vec{x}_s, \vec{x}_i) = \frac{1}{4}\left|\Psi(x_s, y_s; \vec{x}_i) + \Psi(-x_s, -y_s; \vec{x}_i)\right|^2, \text{(6a)}$$

$$P_{b_s,a_i}(\vec{x}_s, \vec{x}_i) = \frac{1}{4}\left|\Psi(x_s, -y_s; \vec{x}_i) - \Psi(-x_s, y_s; \vec{x}_i)\right|^2. \text{(6b)}$$

Therefore, the amount of entanglement of the quantum state given by Eq. (2) can be quantified as $K = (P_+ + P_-)/(P_+ - P_-)$. The experimental setup plotted in Fig. 2 measures the "full" entanglement of the quantum state described by Eqs. (2) or (3).

On the other hand, the joint probability distributions in Eq. (6) also exhibit interesting interference behavior. Using Eq. (3), we have

$$\begin{aligned} P_{\rm diff}(\vec{x}_s, \vec{x}_i) &\equiv P_{a_s,a_i}(\vec{x}_s, \vec{x}_i) - P_{b_s,a_i}(\vec{x}_s, \vec{x}_i) \\ &= \mathcal{N}^2 e^{-R_+(z)(\vec{x}_s^2 + \vec{x}_i^2)} \cos\left[2 I_-(z) \vec{x}_s \cdot \vec{x}_i\right], \quad (7) \end{aligned}$$

where $R_+(z) = w_0^2 / \left[(1 + w_0^4/\sigma_0^2)\gamma(z)\right] + \alpha L / \left[k_p^0 \beta(z)\right]$ and $I_-(z) = \mu_1(z)/\gamma(z) - \mu_2(z)/\beta(z)$. The difference of the joint probability $P_{\rm diff}$ is plotted in Fig. 3 as a function of x_s. It is seen that the location of the second maximum is at $x_s \approx 0.953\pi/x_i I_-$, from which we can determine the entanglement in the phase. That is, the interference of the wave function with itself, with its symmetry, reveals not only the phase information of the wave function, but more importantly how the two photons are correlated in the phase through the fringe pattern given by Eq. (7).

In conclusion, we have demonstrated the Hilbert space migration of entanglement of down-converted photons in free-space propagation. We suggested its implication for experiments involving the quantification of the degree of entanglement by means of common variance measurements. We have also suggested a simple experimental scheme that can detect both the entanglement in amplitude and phase.

KWC acknowledges support from a fellowship from the Croucher Foundation; JPT from the Generalitat de Catalunya, from the European Commission under the integrated project Qubit Applications (QAP) funded by the IST directorate (Contract No. 015848), and from the MEC (Consolider Ingenio 2010 project *QIOT* CSD2006-00019, FIS2004-03556); and JHE from ARO Grant W911NF-05-1-0543. Discussions with R.W. Boyd, C.K.

Law, M.N. O'Sullivan-Hale and K. Wodkiewicz have been very helpful.

Appendix A — Let us consider a bi-photon amplitude that, at the output face of the nonlinear crystal ($z = 0$), is written as

$$\Phi(\vec{p}, \vec{q}) = \left[\frac{\Re(A)\Re(B)}{\pi^2}\right]^{\frac{1}{4}} \exp\Big(-\frac{A|\vec{p}_+|^2 + B|\vec{p}_-|^2}{4}\Big), \quad (8)$$

where $\vec{p}_+ = \vec{p} + \vec{q}$ and $\vec{p}_- = \vec{p} - \vec{q}$. Inspection of Eq. (8) shows that the bi-photon function can be separated for the two transverse dimensions, i.e., $\Phi(\vec{p}, \vec{q}) = \Phi_x(p_x, q_x)\Phi_y(p_y, q_y)$. Therefore, the Schmidt decomposition of Eq. (8) can be written as $\Phi(\vec{p}, \vec{q}) = \sum_{m,n=0}^{\infty} \sqrt{\lambda_{mn}} f_{mn}(\vec{p}) g_{mn}(\vec{q})$, where the basis functions of the decomposition are $f_{mn}(\vec{p}) = \psi_m(p_x)\psi_n(p_y)$ and $g_{mn}(\vec{q}) = \psi_m(q_x)\psi_n(q_y)$, with eigenvalue $\sqrt{\lambda_m \lambda_n}$.

The reduced density matrix for the signal photon, $\rho_s(p_x, p_y, \bar{p}_x, \bar{p}_y,) = \mathrm{Tr}_{\mathrm{idler}} |\Phi\rangle\langle\Phi|$, can be separated into two matrices, i.e., $\rho_s(p_x, p_y, \bar{p}_x, \bar{p}_y,) = \rho_x(p_x, \bar{p}_x)\rho_y(p_y, \bar{p}_y,)$, each one corresponding to a transverse coordinate. The functions ψ_m, and the eigenvalues λ_m can be obtained from the expansion of the one dimensional reduced density matrix ρ_x in the form $\rho_x(p_x, \bar{p}_x) = \sum_{n=0}^{\infty} \lambda_{x,n} \psi_n(p_x)\psi_n(\bar{p}_x)$.

From Eq. (8), the one-dimensional reduced density matrix becomes

$$\rho_x(p_x, \bar{p}_x) = \sqrt{\frac{2\Re(A)\Re(B)}{\pi\Re(A+B)}} \exp\left\{-i\frac{\Im(AB)(p_x^2 - \bar{p}_x^2)}{2\Re(A+B)}\right\} \times \exp\left\{-[(a+b)(p_x^2 + \bar{p}_x^2) - 2bp_x\bar{p}_x]\right\}, \quad (9)$$

where $a = \Re(A)\Re(B)/\Re(A+B)$ and $b = |A - B|^2/[8\Re(A+B)]$. The representation given by Eq. (9) is also found in the determination of the mode structure of Gaussian-Schell model sources in the theory of partial coherence [17]. One can find that the eigenvalue $\lambda_{x,n}$ is given by $\lambda_{x,n} = (a/c)^{1/2}(1 - w^2)^{1/2} w^n$, with $c = (a^2 + 2ab)^{1/2}$ and $w = b/(a+b+c)$. The functions ψ_n are appropriately normalized Hermite-Gaussian functions. Thereafter, the calculation of $K = 1/\sum_{m,n=0}^{\infty} (\lambda_{x,m}\lambda_{y,n})^2$ would yield $K = (c/a)^2$, which can be straightforwardly written as the expression that appears in Eq. (4). Notice that K describes entanglement in the (p_x, p_y) space.

Appendix B — The modified Mach-Zehnder interferometer shown in Fig. 2 contains three basic elements that modify the spatial shape of the bi-photon function. The action of the mirrors is described by $\hat{a}_{in}(x, y) \rightarrow \hat{a}_{out}(x, -y)$, where x and y are the transverse coordinates in the frame of *each* individual beam.

The action of the beam-splitter is [12] $\hat{a}_{in}(x, y) \rightarrow \hat{a}_t(x, y) + i\hat{a}_r(x, -y)$, where $\hat{a}_t$ is the creation operator of the transmitted photon, and $\hat{a}_r$ the corresponding creation operator of the reflected photon. For a Dove prism that is rotated by an angle θ with respect to the axis of image inversion, the fields before and after the dove prism are given by $\hat{a}_{in}(x, y) \rightarrow \hat{a}_{out}(x\cos 2\theta - y\sin 2\theta, -x\sin 2\theta - y\cos 2\theta)$. Together with the effect of the polarization beam-splitter, one thus obtains that all joint probability detections in the configuration described in Fig. 2 are given by Eq. (6).

The bi-photon function at location z can be written in the form

$$\Psi(\vec{r}_s, \vec{r}_i) = \left[\frac{a(1 - w^2)}{c}\right]^{1/2} \sum_{n,m=0}^{\infty} w^{n/2} w^{m/2} \times \psi_m(x_s, z)\psi_n(y_s, z)\psi_m(x_i, z)\psi_n(y_i, z), \quad (10)$$

where the function $\psi_n(x, z)$ corresponds to Hermite-Gaussian function at $z = 0$ that evolves under the sole influence of diffraction. Due to the symmetry of the Hermite-Gaussian functions, one has $\psi_n(-x, z) = (-1)^n \psi_n(x, z)$. Making use of this symmetry property, one obtains

$$P_+ = \frac{a(1 - w^2)}{2c} \left[\sum_{n,m=0}^{\infty} w^{n+m} + (-w)^{n+m}\right]. \quad (11)$$

From Eq. (11), one obtains Eq. (5), taking into account that the amount of entanglement is given by $K = (c/a)^2$.

---

[1] K.W. Chan and J.H. Eberly, arXiv:quant-ph/0404093.

[2] D.C. Burnham and D.L. Weinberg, Phys. Rev. Lett. **25**, 84 (1970).

[3] A. Mair, A. Vaziri, G. Weihs and A. Zeilinger, Nature **412**, 313 (2001).

[4] H.H. Arnaut and G.A. Barbosa, Phys. Rev. Lett. **85**, 286 (2001).

[5] J.T. Barreiro, N.K. Langford, N.A. Peters, and P.G. Kwiat, Phys. Rev. Lett. **95**, 260501 (2005).

[6] J.P. Torres, A. Alexandrescu, and L. Torner, Phys. Rev. A **68**, 050301(R) (2003).

[7] C.K. Law and J.H. Eberly, Phys. Rev. Lett. **92**, 127903 (2004).

[8] J.P. Torres, Y. Deyanova, L. Torner, and G. Molina-Terriza, Phys. Rev. A **67**, 052313 (2003).

[9] M.N. O'Sullivan-Hale, I. Ali Khan, R.W. Boyd, and J.C. Howell, Phys. Rev. Lett. **94**, 220501 (2005).

[10] S. Groblacher, T. Jennewein, A. Vaziri, G. Weihs, and A. Zeilinger, New J. Phys. **8**, 75 (2006).

[11] J.C. Howell, R.S. Bennink, S.J. Bentley, and R.W. Boyd, Phys. Rev. Lett. **92**, 210403 (2004).

[12] S.P. Walborn, A.N. de Oliveira, S. Padua, and C.H. Monken, Phys. Rev. Lett **90**, 143601 (2003).

[13] M.V. Fedorov, M.A. Efremov, P.A. Volkov, E.V. Moreva, S.S. Straupe, and S.P. Kulik, arXiv:quant-ph/0612104.

[14] R. Grobe, K. Rzazewski and J.H. Eberly, J. Phys. B **27**, L503 (1994).

[15] A. Ekert and P.L. Knight, Am. J. Phys. **63**, 415 (1995).

[16] M.V. Fedorov, M.A. Efremov, A.E. Kazakov, K.W. Chan, C.K. Law, and J.H. Eberly, Phys. Rev. A **72**,

032110 (2005).
[17] A. Starikov and E. Wolf, J. Opt. Soc. Am. **72**, 923 (1982).